*Anal. Chem.* **2000,** *72,* 5143−5150

*Accelerated Articles*

# Molecular Dynamics Simulation of the Laser Disintegration of Aerosol Particles

Tracy A. Schoolcraft,[†] Gregory S. Constable,[†] Leonid V. Zhigilei,[‡,§] and Barbara J. Garrison*[,‡]

*Department of Chemistry, Shippensburg University, 1871 Old Main Drive, Shippensburg, Pennsylvania 17257, Department of Chemistry, 152 Davey Laboratory, The Pennsylvania State University, University Park, Pennsylvania 16802, and Department of Materials Science and Engineering, University of Virginia, Thornton Hall, Charlottesville, Virginia 22903*

**The mechanisms of disintegration of submicrometer particles irradiated by short laser pulses are studied by a molecular dynamics simulation technique. Simulations at different laser fluences are performed for particles with homogeneous composition and particles with transparent inclusions. Spatially nonuniform deposition of laser energy is found to play a major role in defining the character and the extent of disintegration. The processes that contribute to the disintegration include overheating and explosive decomposition of the illuminated side of the particle, spallation of the backside of large particles, and disruption of the transparent inclusion caused by the relaxation of the laser-induced pressure. The observed mechanisms are related to the nature of the disintegration products and implications of the simulation results for aerosol time-of-flight mass spectrometry are discussed. Application of multiple laser pulses is predicted to be advantageous for efficient mass spectrometry sampling of aerosols with a large size to laser penetration depth ratio.**

An increasing need for the development of quantitative methods for aerosol characterization is driven by the recognition of the importance of natural and anthropogenic aerosol particles for atmospheric chemistry and public health. Particulate matter is responsible for heterogeneous chemical reactions in the atmosphere and plays an important role in stratospheric ozone depletion.[1] Aerosol particles have also been correlated to adverse heath effects such as respiratory diseases.[2] There is evidence that small submicrometer particles are more reactive and more dangerous then larger particles due to a larger surface-to-volume ratio and higher permeability into the respiratory system.[3]

Recent advances in the analytical aerosol characterization are largely coming from a quickly expanding field of aerosol mass spectrometry (MS).[4] In particular, a new aerosol time-of-flight mass spectrometry (ATOFMS) technique developed by Prather et al.[5,6] provides an efficient method for real-time simultaneous measurement of size and chemical composition of individual particles. This method has been used to reveal important size−composition correlations for ambient aerosol particles in atmospheric systems.[7,8]

Among different ionization techniques used in aerosol MS, laser desorption/ionization has many advantages[4] and is the method of choice in real-time single-particle mass spectrometry techniques, such as ATOFMS. In this method, short pulse laser irradiation is focused on a single aerosol particle and leads to the partial or complete disintegration of the particle. Some of the species present in the particle can be ionized by the same pulse and elemental, molecular, and isotopic MS analysis can be performed. To obtain an accurate and complete chemical fingerprint, the aerosol particle has to be uniformly disintegrated into the constituent molecules. On the other hand, the chance of fragmentation of molecules present in the particle increases with the amount of the energy deposited by the laser pulse and limits the range of useful laser fluences. Optimization of irradiation

[†] Shippensburg University.
[‡] The Pennsylvania State University.
[§] University of Virginia.

(1) Hamill, P.; Toon, O. B. *Phys. Today* **1991**, *44*, 34−42.
(2) Dockery, D. W.; Pope, C. A., III *Annu. Rev. Public Health* **1994**, *15*, 107−132.
(3) Hinds, W. C. *Aerosol Technology−Properties, Behavior, and Measurement of Airborne Particles*; John Wiley & Sons: New York, 1982.
(4) Suess, D. T.; Prather, K. A. *Chem. Rev.* **1999**, *99*, 3007−3035.
(5) Salt, K.; Noble C. A.; Prather, K. A. *Anal. Chem.* **1996**, *68*, 230−234.
(6) Liu, D. Y.; Rutherford, D.; Kinsey, M.; Prather, K. A. *Anal. Chem.* **1997**, *69*, 1808−1814.
(7) Noble, C. A.; Prather K. A. *Environ. Sci. Technol.* **1996**, *30*, 2667−2680.
(8) Allen, J. O.; Fergenson, D. P.; Gard, E. E.; Hughes, L. S.; Morrical, B. D.; Kleeman, M. J.; Gross, D. S.; Gälli, M. E.; Prather, K. A.; Cass, G. R. *Environ. Sci. Technol.* **2000**, *34*, 211−217.

10.1021/ac0007635 CCC: $19.00 
Published on Web 09/30/2000

parameters and adequate interpretation of MS experimental data require a thorough understanding of the laser-induced processes in the irradiated particle. The processes leading to the particle disintegration can be rather complex and, depending on the irradiation conditions and properties of the particle material, can involve thermal,[9−11] photochemical, photomechanical,[9,11] and electronic[10] effects. The question of a relative contribution of these effects and their relation to the final disintegration products still remains unanswered even at a qualitative level.

A method that is capable of providing a detailed microscopic picture of the dynamic processes induced by the laser pulse is the molecular dynamics (MD) computer simulation technique.[12,13] The direct application of the atomistic MD approach to the laser ablation phenomenon, however, is hampered by relatively large sizes of aerosol particles and a collective character of the processes leading to the particle disintegration. Recent development of a coarse-grained breathing sphere MD model,[14] where a group of atoms rather than each atom is treated as a unit, has significantly expanded the time and length scales accessible for the simulations.[15] The model has been successful in computational investigation of mechanisms of laser ablation of organic solids and matrix-assisted laser desorption/ionization (MALDI).[14,15] In addition, initial simulations of laser interaction with individual submicrometer particles have been reported for the case when laser energy is uniformly deposited within the particle.[11] A strong pulse width dependence of the mechanisms of particle disintegration has been revealed in these simulations. An explosive thermal decomposition was found to be characteristic for longer laser pulses whereas mechanical disruption of the particle driven by the relaxation of the laser-induced pressure was observed for shorter laser pulses, in the regime of stress confinement. Uniform energy deposition simulated in ref 11 corresponds to the case when the size of the particle is much smaller than the optical penetration depth of the material making up the aerosol particle. In the present work, we extend this initial study to more complex cases of (1) highly absorbing particles, when the optical penetration depth is less or comparable to the size of the particle, and (2) heterogeneous aerosols, composed of absorbing and optically transparent components.

The aim of this work is to provide a qualitative understanding of the effect of a spatially nonuniform deposition of laser energy on the mechanisms of particle disintegration and the nature of the final disintegration products. A discussion of implications of the simulation results for aerosol mass spectrometry applications is also presented.

## COMPUTATIONAL MODEL

The breathing sphere model for molecular dynamics simulations has been used extensively to investigate the laser desorption/ablation process[11,15] and has been presented in detail elsewhere.[14] Briefly, each molecule in the system is represented by a single particle with true translational degrees of freedom but one approximate internal degree of freedom. This internal degree of freedom allows us to reproduce a realistic rate for the conversion of the internal energy of the molecules excited by the laser irradiation to the translational motion of the molecules. The parameters of the intermolecular potential are chosen to represent the van der Waals interactions in a molecular solid. A mass of 100 Da is attributed to each molecule. The parameters of the internal potential are chosen to provide a characteristic time of the vibrational relaxation of an excited molecule to be on the order of 10 ps, a value typical for organic solids.[16]

We have chosen to use a two-dimensional (2D) version of the breathing sphere model as it offers a clear visual picture of laser-induced processes[11,14] and gives the same qualitative results as the three-dimensional model[14] in considerably shorter computer time. To examine the effect of the size of aerosol particle on the disintegration process, simulations are performed for particles of two different sizes. The smaller particle has diameter of 50 nm and contains 6829 molecules; the larger one has a diameter of 110 nm and contains 33 799 molecules.

In addition to the simulations performed for particles of uniform composition, a series of simulations is performed to explore the basic mechanisms of laser interaction with heterogeneous aerosol particles composed of absorbing and optically transparent components. As a simple model for heterogeneous aerosols, we consider particles containing two types of molecules, absorbing and nonabsorbing, with the nonabsorbing molecules located in the core. Simulations are performed for particles with a diameter of 110 nm and three different diameters of the core, 25, 50, and 75 nm, referred to as small, medium, and large, respectively. Simulations for particles with an absorbing core and a transparent periphery are in progress and will be presented elsewhere.[17]

The laser irradiation is simulated by vibrational excitation of molecules that are randomly chosen during the laser pulse duration of 15 ps. The vibrational excitation is modeled by depositing a quantum of energy equal to the photon energy into the kinetic energy of internal motion of a molecule to be excited. Irradiation at a wavelength of 337 nm (3.68 eV) is simulated in this study, but the photon energy deposited is scaled down by a half to account for the lower binding energy of the 2D system as compared to the three-dimensional (3D) system. The probability of molecules to be excited is modulated by Lambert−Beer's law to reproduce the exponential attenuation of the laser light with depth. An absorption depth of 25 nm is used in the simulations. Thus, the ratios of the diameter of the particle to the absorption depth are 2 and 4.4 for the small and large particles, respectively. The density of the absorbed laser energy within the particle depends on the distance from the surface of the particle in the direction of the incident laser pulse. The resulting distribution of absorbed energy density is shown schematically in Figure 1a. In simulations of particles with a transparent core, the molecules that belong to the core do not absorb photons and do not contribute to the attenuation of the laser light. This results in a


(9) Kafalas, P.; Ferdinand, A. P., Jr. *Appl. Opt.* **1973**, *12*, 29−33.
(10) Heinen, H. J. *Int. J. Mass Spectrom. Ion Phys.* **1981**, *38*, 309−322.
(11) Zhigilei, L. V.; Garrison, B. J. *Appl. Surf. Sci.* **1998**, *127−129*, 142−150.
(12) A. Vertes, A. Bencsura, M. Sadeghi and X. Wu, *Proc. SPIE-Int. Soc. Opt. Eng.* **2000**, *3935*, 76−84.
(13) Dutkiewicz, Ł.; Johnson, R. E.; Vertes, A.; Pędrys, R. *J. Phys. Chem. A* **1999**, *103*, 2925−2933.
(14) Zhigilei, L. V.; Kodali, P. B. S.; Garrison, B. J. *J. Phys. Chem. B* **1997**, *101*, 2028−2037. Zhigilei, L. V.; Kodali, P. B. S.; Garrison, B. J. *J. Phys. Chem. B* **1998**, *102*, 2845−2853.
(15) Zhigilei, L. V.; Garrison, B. J. *Appl. Phys. Lett.* **1999**, *74*, 1341−1343. Zhigilei, L. V.; Garrison, B. J. *Appl. Phys. A* **1999**, *69*, S75−S80. Zhigilei, L. V.; Garrison, B. J. *J. Appl. Phys.* **2000**, *88*, 1281−1298.
(16) Chang, T.-C.; Dlott, D. *J. Chem. Phys.* **1989**, *90*, 3590.
(17) Schoolcraft, T. A.; Constable, G. S.; Jackson, B.; Zhigilei, L. V.; Garrison, B. J. *Nucl. Instrum. Methods B*, in press.

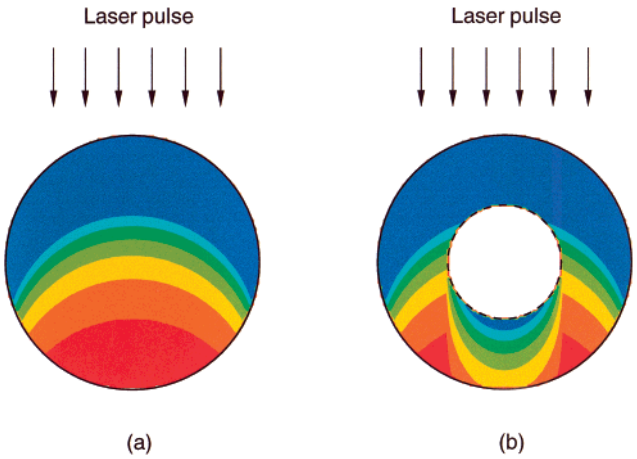


Figure 1. Schematic drawing of the energy density distribution in a homogeneous absorbing particle (a) and a particle with a transparent inclusion (b) irradiated by a laser pulse. The energy density is the highest in the blue areas and the lowest in the red areas. The transparent inclusion is marked by the dashed line. For the circular geometry, the distance $z = 0$ for Beer's law is the semicircular front edge of the particle. The size of the particle is 110 nm with a 50-nm core for frame b.

more complex distribution of the energy density in the irradiated particle, as shown in Figure 1b.

The total number of photons entering the model during the laser pulse is determined by the laser fluence. Because the particles have finite depth, not all incident photons are absorbed by the particle; thus, in addition to the incident fluence, we also state the energy deposited to the particle at the frontside and the backside. Simulations are performed for a range of laser fluences, from 25 to 500 eV/nm. Since the system is two-dimensional, the fluence has units that are different from the conventional ones and the values of laser fluence used in the simulations cannot be related to the experimental values.

## RESULTS

Simulations at different laser fluences are performed for particles with homogeneous composition and particles with a transparent inclusion. A qualitative discussion of the character of particle disintegration is based on the visual analysis of the snapshots from the simulations. Calculation of energy density and pressure distributions in the particles at different times following irradiation by the laser pulse is used to provide a physical interpretation of the visual pictures. In the next subsection, the results for homogeneous particles are given and the dependence of the extent of disintegration on laser fluence and the ratio of particle size to absorption depth are discussed. The results for the particles with a transparent inclusion of different sizes are presented in subsection 2, and the discussion of the implications of the simulation results for aerosol mass spectrometry is given in subection 3.

**1. Laser Fluence and Particle Size Dependence for Homogeneous Particles.** To perform a qualitative analysis of the fluence and particle size dependence of the disintegration process, six representative simulations are chosen for discussion in this section. The first two simulations are for the lowest laser fluence studied, 25 eV/nm. At this fluence, the result for each particle size is nearly identical; namely, a material ejection (or ablation) occurs at the frontside of the particle as shown in Figure 2. Increasing the laser fluence to 100 eV/nm almost fully disintegrates the small particle whereas the large particle still experiences only ablation at the frontside as shown in Figure 3. In all four cases examined so far, even when there is considerable disintegration, the material is not completely dissociated into individual molecules. Some clusters or chunks of the original particle remain intact. The last two simulations were performed using a higher laser fluence, 300 eV/nm. As would be expected, the increase in fluence leads to a more complete disintegration of the small particle with no clusters observed in the snapshot taken at 400 ps after the start of the simulation, Figure 4a. The large particle, however, has experienced something beyond ablation. The backside of the particle, which remained intact using the lower laser fluences, is now fractured into several large pieces, Figure 4b.

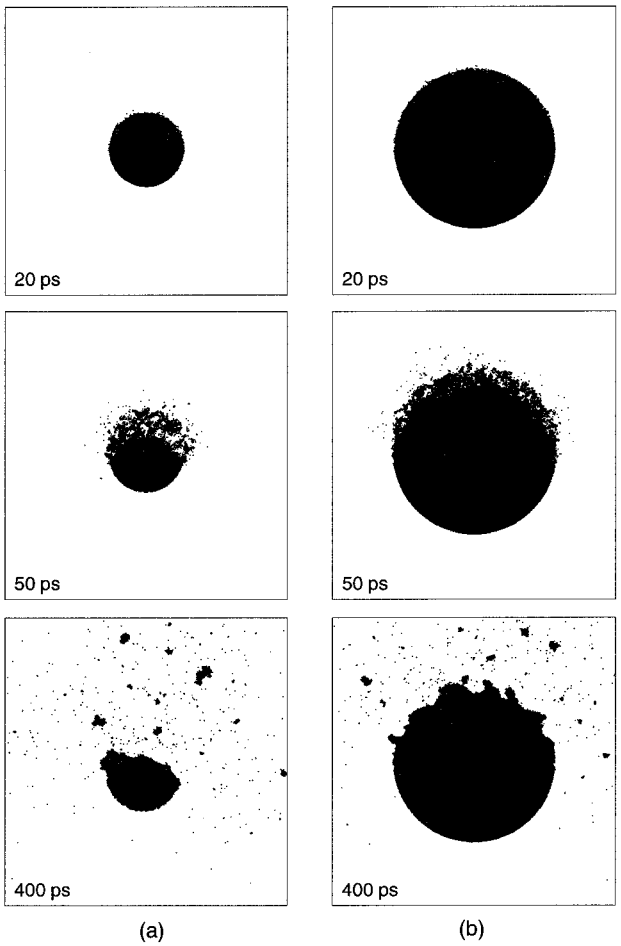


Figure 2. Snapshots from the simulations of laser irradiation of small, 50 nm in diameter, particle (a) and large, 110 nm in diameter, particle (b). The laser penetration depth is 25 nm, the pulse duration is 15 ps, and the laser fluence is 25 eV/nm. Snapshots are shown for times 20, 50, and 400 ps after the start of the laser pulse.

To obtain insight into the qualitative pictures described above, we calculate the energy density deposited into the particle by the laser pulse and compare the results to the conclusions from earlier simulations and a simple model relating the amount of ablated material to laser fluence. In recent 3D simulations of laser ablation of organic solids,[15] we have shown that the ablation depth follows the laser energy deposition and all material that absorbs an energy

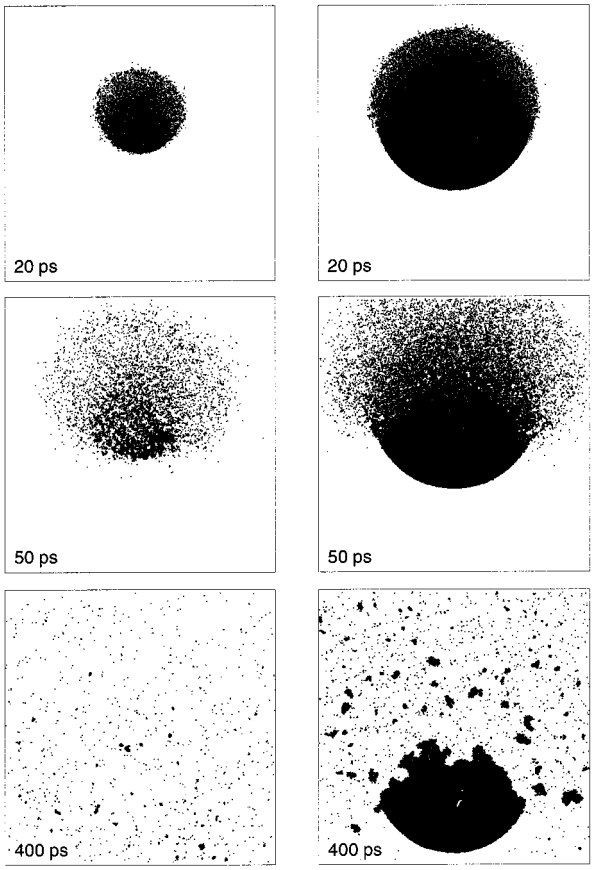


Figure 3. Same as in Figure 2, but for a laser fluence of 100 eV/nm.

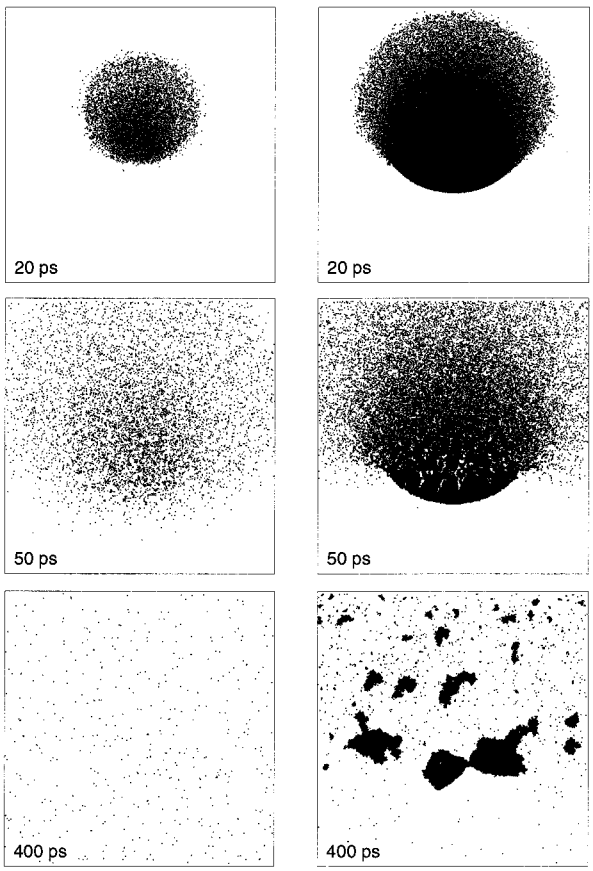


Figure 4. Same as in Figure 2, but for a laser fluence of 300 eV/nm. The area shown in the snapshots taken at 400 ps is shifted down by 200 nm to show the clusters in (b) that are moving with velocity of ~500 m/s in the direction of the laser pulse.

density higher than a critical energy density $E_v$* is ablated. This observation agrees with prediction of a model proposed for MALDI[18] and with experimental observations for polymer ablation.[19] This model has been quantitatively applied to bulk samples with flat surfaces. In the case of the present simulations, because of the round geometry and limited number of fluences investigated, we can only qualitatively apply the model to estimate what part of the particle is ablated at a given laser fluence. With an exponential decay of laser intensity given by Beer's law, the energy density $E_v$ deposited at a depth $z$ under the surface is $E_v = F/L_p \exp[-z/L_p]$, where $F$ is the fluence at the surface, $z = 0$, and $L_p$ is the laser penetration depth. For the circular geometry, the $z = 0$ position follows the front edge of the particle. The energy density reached at the surface of the particle is $E_0 = F/L_p$ and the fraction of the particle to be ablated, $z^*/d$, can be estimated as

$$z^*/d = L_p/d \ln(E_0/E_v^*) \quad (1)$$

where $d$ is the diameter of the particle. A fit of the simulation results to eq 1 gives a value of $E_v^* \approx 0.2$ eV/molecule. This value is slightly higher than the values found in previous 2D simulations for flat surfaces (~0.17 eV/molecule)[20] and for particles (~0.14 eV/molecule in the regime of stress confinement and ~0.19 eV/molecule in the regime of thermal confinement).[11] The discrepancy in the threshold energies can be explained by different geometries of the samples and by a uniform rather than Beer's law energy deposition used in the earlier simulations.

The dependence of the ablation process on the size of the particle is examined first for the lowest laser fluence, 25 eV/nm. Figure 2 shows snapshots for the small and large particles at 20, 50, and 400 ps. On average, both particles receive an energy density of 0.3 eV/molecule at the front of the particle. Equation 1 predicts that about 20% of the small particle and 9% of the large particle should ablate, values in good agreement with the values of 23 and 4% from the simulations. The backsides of both particles remain intact.

For a higher laser fluence of 100 eV/nm, the effect of the size of the particle is more dramatic, Figure 3. For the small particle, we observe a complete dissociation into individual molecules and small clusters, Figure 3a, whereas the large particle still only experiences frontside ablation leaving the backside virtually intact, Figure 3b. There is a good qualitative agreement between these observations and the model discussed above. Equation 1 predicts that 90 and 41% of the small and large particles, respectively,

(18) Johnson, R. E. In *Large Ions*: *Their Vaporization, Detection and Structural Analysis*; Baer, T., Ng, C. Y., Powis, I., Eds.; John Wiley & Sons: New York, 1996; pp 49−77.

(19) Srinivasan, R.; Braren, B. *Chem. Rev.* **1989**, *89*, 1303−1316.

(20) Zhigilei, L. V.; Kodali, P. B. S.; Garrison, B. J. *Chem. Phys. Lett.* **1997**, *276*, 269−273.

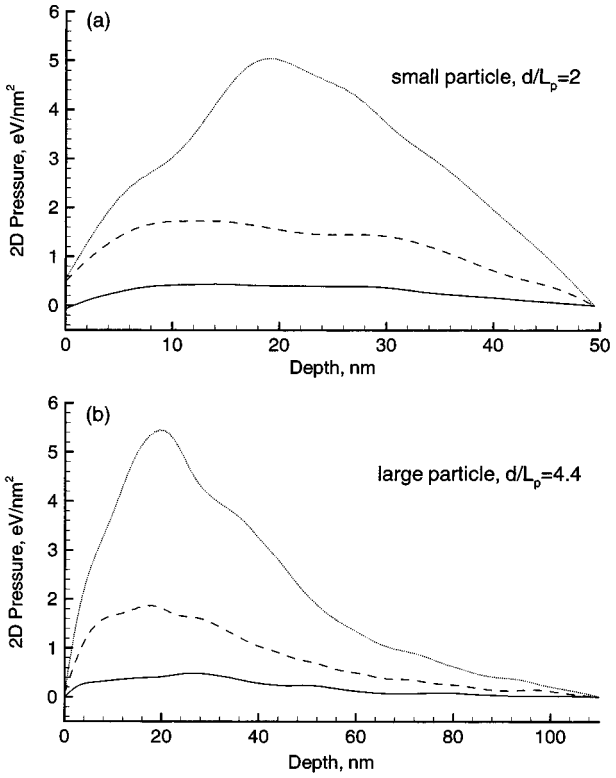


Figure 5. 2D pressure versus depth into the particle for the small particle (a) and the large particle (b). The pressure is averaged for the middle 10% of the particles at 10 ps after the start of the laser pulse. Zero value of the depth corresponds to the front edge of the illuminated side of the particle. The solid, dashed, and dotted lines are for the simulations with laser fluences of 25, 100, and 300 eV/nm, respectively.

should ablate, thus leaving small clusters for the small particle, Figure 3a, and over a half of the large particle, Figure 3b.

Figure 4 shows the result of an additional increase of the laser fluence up to 300 eV/nm. Here the small particle is completely disintegrated, Figure 4a. Ninety-four percent of the particle exists as individual molecules, and at the end of the simulation, there are no clusters that contain more than six molecules. In fact, the fluence is sufficiently high for multiphoton absorption to occur and photofragmentation of individual molecules can be expected in the real situation. Still, for the large particle, eq 1 predicts that only about two-thirds of the particle will be ablated even at this high fluence. Although it is difficult to determine from Figure 4b how much is not ablated, the largest cluster remaining is 16% of the original particle and there are several other large clusters remaining.

The increase in the laser fluence not only causes ablation of an increasingly larger part of the particles but also leads to the higher expansion velocities of the ejected plume, Figures 2−4. The expansion velocities can be related to the values of the compressive pressure that builds up in the absorption region of the irradiated particle during the laser pulse. A strong fluence and particle size dependence of both the position and the maximum values of the laser-induced pressure is apparent from the pressure distributions given in Figure 5. The relaxation of the higher pressure leads to the higher ejection velocities. In the case of the large particle, the maximum of the initial pressure distribution is located near the frontside of the particle, Figure 5b. Relaxation of the pressure in this case not only causes forwarded ejection of the ablation plume but also can drive a strong pressure wave through the particle. Reflection of the pressure wave from the back surface leads to the development of the tensile stresses that can fracture the backside of the particle, Figure 4b. A similar mechanism of pressure-driven particle fragmentation has been proposed as a possible explanation for experimentally observed fragmentation of the backside of irradiated water droplets.[9]

Snapshots from the simulations that show the expansion of the ablation products, Figures 2−4, can be qualitatively related to experimental time-resolved photographs taken during laser vaporization and fragmentation of small water droplets.[9,21] An asymmetric ejection of the ablation products from the illuminated side has been observed for droplets with radius larger than the laser penetration depth. Experimental photographs in this case[9,21] are similar to the snapshots from the present simulations for the large particle, Figures 3b and 4b. For smaller droplets, with radius close to the penetration depth, the expanding plume is nearly symmetric and the entire droplet disappears as time progresses.[9] These observations can be related to the simulation for the small particle and high fluence, Figure 4a, when a complete vaporization of the particle is observed, as well as to the earlier simulations with a uniform absorption of the laser energy within the particle.[11]

**2. Laser Disintegration of Particle with a Transparent Inclusion.** To study the effect of a transparent inclusion on the mechanism of the particle disintegration, we performed simulations of laser irradiation of particles that contain a transparent core of three different sizes, small (23% of the particle diameter), medium (45%), and large (68%). In this section, we first discuss the dependence of the character of particle disintegration on laser fluence. In this discussion, the results for particles with an inclusion of the medium size are used. The effect of the size of the transparent inclusion is then investigated, and the mechanisms leading to disintegration of the inclusion are discussed.

Snapshots from the simulations for particle with the medium size inclusion are shown in Figure 6 for three different fluences. For the lowest laser fluence, 25 eV/nm, the visual picture of laser ablation is similar to the one for the homogeneous particle at the same fluence, Figure 2b. Most of the laser energy is absorbed in the top layer of the particle, and the transparent inclusion does not significantly affect the final distribution of energy deposited by the laser pulse.

As fluence increases to 100 eV/nm, the effect of the transparent inclusion starts to show up more apparently, Figure 6b. According to eq 1, the ablation depth for this fluence is 41% of the particle diameter. In the case of a particle with a transparent inclusion, this means that the critical energy density of 0.2 eV/molecule is reached not only in the frontside region but also beneath the inclusion. In the backside of the particle, however, the overheated region is trapped between the transparent inclusion and a colder region near the back surface of the particle. The relaxation of the trapped overheated region leads to the disruption of the backside of the particle rather than ablation, Figure 6b. The presence of a thin layer of the absorbing material that remained at the frontside of the particle at the end of the

(21) Wood, C. F.; Leach, D. H.; Zhang, J.-Z.; Chang, R. K.; Barber, P. W. *Appl. Opt.* **1988**, *27*, 2279−2286.

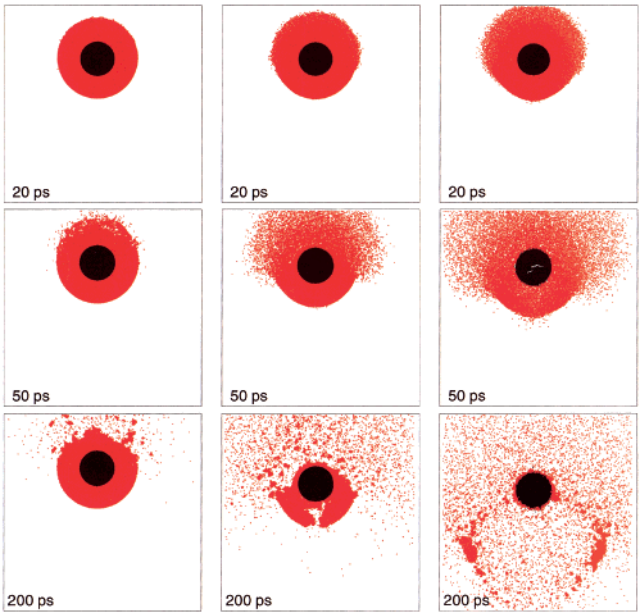


Figure 6. Snapshots from the simulations of laser irradiation of particle with a transparent inclusion of medium (45% of the particle diameter) inclusion. Snapshots are shown for times 20, 50, and 200 ps after the start of the laser pulse. Simulations are performed with laser fluences of (a) 25, (b) 100 , and (c) 300 eV/nm. Absorbing molecules are red; molecules that belong to the transparent inclusion are black.

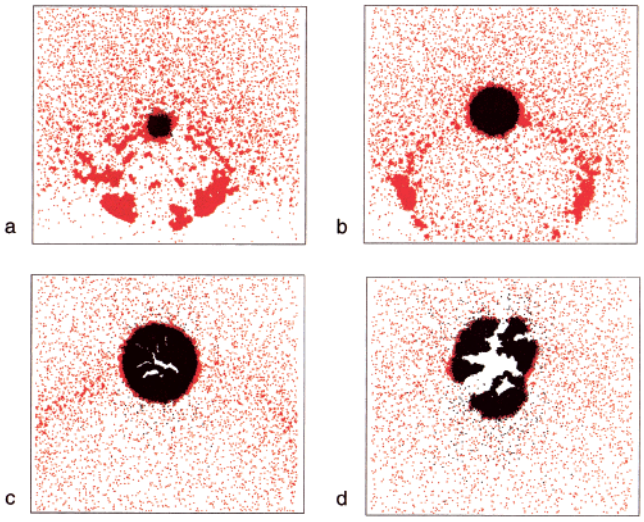


Figure 7. Snapshots from simulations performed for particles with transparent inclusion of three different sizes, (a) small (23% of the particle diameter), (b) medium (45%), and (c, d) large (68%). A laser fluence of 300 eV/nm is used in the simulations illustrated by snapshots in (a−c) and 500 eV/nm in (d). Snapshots are shown for 200 ps after the start of the laser pulse. Absorbing molecules are red; molecules that belong to the transparent inclusion are black.

simulation can be attributed to the thermal conduction to the transparent inclusion.

At the laser fluence of 300 eV/nm, the absorbing component of the particle is completely disintegrated, Figure 6c. Although the major part of the absorbing component decomposes into individual molecules, a few relatively large clusters are also observed at the end of the simulation, Figure 6c. These clusters originate from the sides of the particle where the deposited energy density is the lowest, Figure 1b.

Although virtually all absorbing molecules have been stripped off the transparent inclusion by the laser pulse at 300 eV/nm, only a few molecules that belong to the inclusion have been ejected. Apparently the ablation process is too fast for the thermal conduction to transfer a significant part of the deposited laser energy to the transparent inclusion. Another effect observed in this simulation is generation and disappearance of microcracks in the central part of the inclusion. In Figure 6c, the microcracks are visible at 50 ps but disappear by the end of the simulation. The effect of microcrack generation is caused by focusing of the laser-induced pressure wave within the transparent inclusion and, as demonstrated below, becomes more pronounced for larger inclusions.

The dependence of the particle disintegration process on the size of the transparent inclusion is illustrated by Figure 7a−c, where snapshots from simulations performed at the same laser fluence of 300 eV/nm and three different sizes of the inclusion are shown. More efficient dissociation of the absorbing component of the particle into individual molecules is observed for particles with larger inclusions. This observation is not surprising since the amount of energy deposited in the backside of the particle is increasing with the size of the inclusion. A less anticipated observation is the onset of the internal fracture as the size of the inclusion increases, Figure 7c. For the same laser fluence of 300 eV/nm there is no crack nucleation in the small inclusion, Figure 7a, only temporal appearance of the cracks is observed in the medium inclusion, Figure 6c, and relatively large cracks that do not disappear with time are produced in the large inclusion, Figure 7c. An additional increase of the laser fluence leads to a more substantial damage to the inclusion, as shown for a fluence of 500 eV/nm in Figure 7d. In this case, the microcracks crop out to the surface of the inclusion and split it apart.

To reveal the physical processes that are responsible for the crack generation, we perform an analysis of the spatial and time development of the local pressure for two simulations illustrated by snapshots in Figure 7a and c. The pressure distributions are presented in the form of contour plots in Figure 8. In both simulations, a high compressive pressure (positive pressure in Figure 8) builds up in the absorption region. This pressure is the result of the rapid temperature increase that occurs on the time scale of the laser pulse. In the case of the small inclusion, the absorption is localized in the frontside of the particle and the initial pressure distribution follows the energy deposition, Figure 8a. Relaxation of the initial pressure in this case drives a pressure wave through the particle. As discussed above for homogeneous particles, interaction of the pressure wave with the back surface can contribute to the fragmentation and ejection of the backside of the particle but the pressure passage does not inflict any damage on the inclusion.

The situation is rather different in the case of the large inclusion. A significant part of the energy of the laser pulse reaches the backside of the particle and the initial pressure is created on both sides of the inclusion, Figure 8b. This initial pressure as well as the ablation recoil pressure caused by the ejection of the absorbing shell drives the compressive pressure wave from both sides of the inclusion. By 20 ps, the pressure wave focuses within the inclusion leading to the pressure spike that is significantly

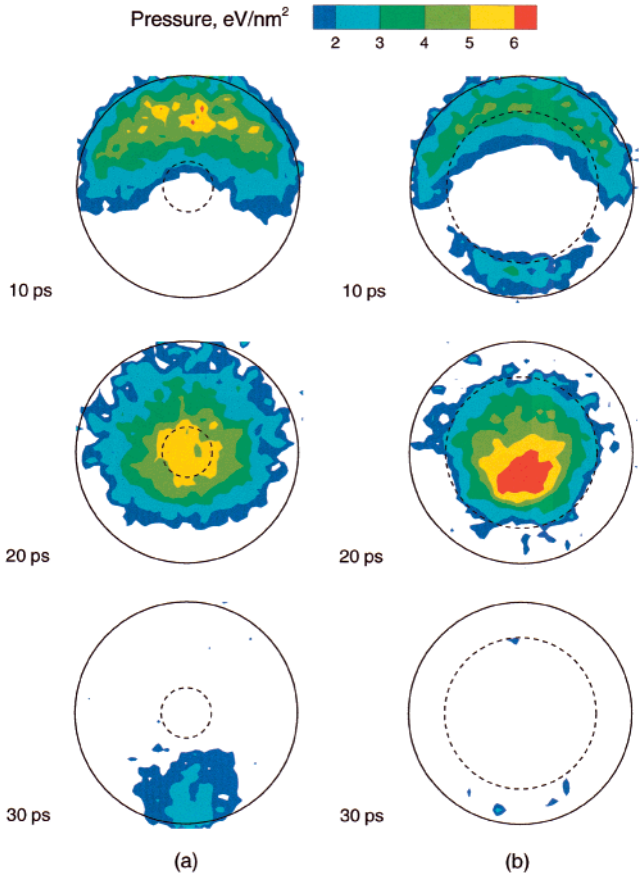


Figure 8. Spatial distribution of the 2D pressure within the particles that contain small (a) and large (b) transparent inclusions. Simulations are performed at a laser fluence of 300 eV/nm. The solid and dashed circles show the original boundaries of the particles and inclusions, respectively.

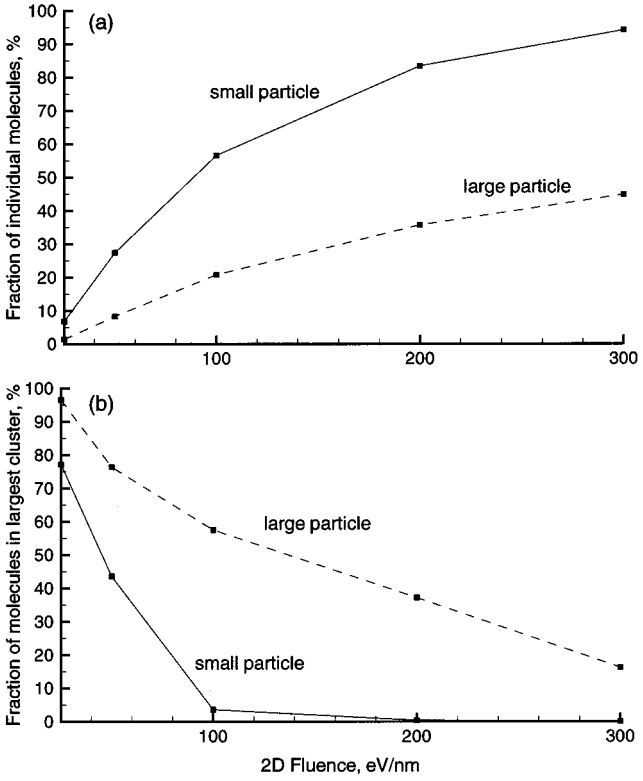


Figure 9. Fraction of individual molecules (a) and molecules in the largest cluster (b) calculated at the end of the simulations, 400 ps, for different laser fluences.

higher than the initial pressure, Figure 8b. The high compressive pressure leads to the expansion of the inclusion with tensile stresses concentrated in the central part of the inclusion. The tensile stresses can be sufficiently high to cause internal fracturing and, at high laser fluence, disintegration of the inclusion, Figure 7c,d.

**3. Implications for Aerosol Mass Spectrometry.** Quantitative MS analysis of aerosols requires clear understanding of the mechanisms of particle disintegration and the nature of disintegration products for different particle sizes and morphologies. A range of homogeneous and multicomponent aerosols of different sizes should be considered when ambient atmospheric particles are of interest.[4] Simulations discussed in the present work provide a basic qualitative understanding of the disintegration processes for simple models of homogeneous strongly absorbing particles and a two-component particle with a transparent inclusion. The discussion of the efficiency of disintegration for these models is given below.

To quantify the efficiency of disintegration, the fraction of the irradiated particle that decomposes into individual molecules is given in Figure 9a for the small and large particles with homogeneous composition. In addition, the number of molecules in the largest cluster remaining at the end of the simulation is determined and expressed as a fraction of the total number of particles in the original cluster, Figure 9b. It is apparent from these graphs that the efficiency of dissociation to individual molecules is much higher and the dependence on the laser fluence is much stronger for the small particles as compared to the large particles. The slow increase of the fraction of individual molecules in the case of the large particle can be correlated to the weak logarithmic dependence of the ablation depth on laser fluence given by eq 1. As the ratio of the particle size to the absorption depth becomes large ($\geq 2$), a complete disintegration can be achieved only at very high fluences, when intensive multiphoton absorption and photofragmentation of molecules at the frontside of the particle can be expected.

On the basis of this analysis, we suggest that several pulses at a lower laser fluence can be more efficient in disintegrating an aerosol particle than one pulse at a higher fluence. With each pulse, the ratio of the remaining particle's diameter to the absorption depth will become smaller, leading to increasingly efficient dissociation into individual molecules with less photofragmentation. For example, in the simulation shown in Figure 3b, over half of the large particle is ablating at a fluence of 100 eV/nm. One can expect that irradiation with the second pulse of the same fluence would produce the result close to the one shown in Figure 3a for the small particle, when more than 50% of the original particle are existing as individual molecules. We estimate that generation of the same number of individual molecules from the large particle by a single laser pulse would require laser fluence higher than 400 eV/nm. Even though the total energy delivered by two pulses at 100 eV/nm is twice lower than the energy of one pulse at 400 eV/nm, the application of the two pulses should be more efficient at creating a representative sampling for MS analysis.

If an absorbing particle contains a transparent inclusion, the efficiency of decomposition of the absorbing component into individual molecules increases. At the same time, the only mechanism of disintegration observed for inclusions is the mechanical fracture caused by the relaxation of the laser-induced pressure. With this mechanism, an inclusion can break up into large pieces but virtually no individual molecules are produced from the transparent component for MS sampling. To sample the inclusions or regions of particles with different absorption spectra, a second laser pulse with wavelength tuned to the absorption of the inclusion material should be used. An alternative way for volatilization of a transparent inclusion is to apply a longer laser pulse, when the thermal conduction from the hot absorbing material heats the transparent material during the pulse duration. The pulse duration in this case should be longer than the time of the heating of the transparent inclusion by thermal conduction from the absorbing region, $\tau_{th} \sim R_{incl}^2/D_T$, where $D_T$ is the thermal diffusivity of the material and $R_{incl}$ is the radius of the inclusion. A potential problem in this case could be the thermal dissociation of organic molecules.

Simulation results presented in this work provide qualitative information on the effect of a spatially nonuniform deposition of laser energy in homogeneous particles and particles with a transparent inclusion. Taken together with simulations for uniform energy deposition,[11] and more recent simulations for particles with an absorbing core and a transparent periphery,[17] the present work gives a consistent qualitative picture of the basic mechanisms of laser interaction with homogeneous and two-component particles. The simulations for the two-component model can be related to such systems as quartz particles mixed internally with aerosols from coal mine dusts[22] or particles with an inorganic core of ammonium sulfate covered with an organic layer originating from car exhaust emission.[23] In general, atmospheric aerosol particles can have a wide spectrum of optical, mechanical, and thermal properties as well as a variety of compositions and structural organization. The MD simulations allow us to view the diversity of processes responsible for laser-induced disintegration of aerosol particles and to set up an initial stage for interpretation of aerosol MS experimental data.

(22) Tourmann, J. L.; Kaufmann, R. *Int. J. Environ. Anal. Chem.* **1993**, *52*, 215−227.
(23) Goshnick, J.; Fichtner, M.; Lipp, M.; Schuricht, J.; Ache, H. J. *Appl. Surf. Sci.* **1993**, *70*, 63−67.

## ACKNOWLEDGMENT

T.A.S. thanks the Shippensburg University Professional Development Committee and the National Science Foundation for providing travel funds and a summer stipend in order for this work to be performed. Partial support of this work was provided by the United States Office of Naval Research through the Medical Free Electron Laser Program and the National Science Foundation through the Chemistry Division. The computational support was provided by IBM through the Selected University Research Program, the National Science Foundation through the MRI Program, and the Center for Academic Computing at The Pennsylvania State University.

Received for review July 5, 2000. Accepted September 11, 2000.

AC0007635